J. Fluid Mech. (2001), *vol.* 433, *pp.* 61–75. Printed in the United Kingdom

The generation of internal waves by vibrating elliptic cylinders. Part 3. Angular oscillations and comparison of theory with recent experimental observations

By D. G. HURLEY† AND M. J. HOOD

Department of Mathematics and Statistics, University of Western Australia, Nedlands WA 6009, Australia

(Received 28 September 1998 and in revised form 26 September 2000)

In this paper the methods of Parts 1 and 2 are extended to the case when the elliptic cylinder is executing angular oscillations about its centreline. At large distances from the cylinder the solution for a beam of waves tends to a similarity solution that decays more rapidly with distance than does the similarity solution for rectilinear oscillations described in Thomas & Stevenson (1972). Figure 4 shows in a remarkable way how the predicted wave profiles change with distance from the inviscid solution to the similarity one.

In the latter part of the paper the predictions of Parts 1 and 2 and other theories are compared with recent experimental observations. The results of the experiments are in good agreement with the predictions of Parts 1 and 2.

1. Introduction and summary

The generation of internal gravity waves by an elliptic cylinder performing rectilinear oscillations in a slightly viscous Boussinesq fluid whose Brunt–Väisälä frequency N is constant was investigated in Hurley (1997) and Hurley & Keady (1997), hereafter referred to as Parts 1 and 2 respectively. In §§ 2 to 5 of the present paper we investigate the waves that are produced when the cylinder is performing angular oscillations about its centreline. As well as having intrinsic interest, the results obtained may be useful to experimenters as 'paddles' executing angular oscillations are popular for generating internal waves in the laboratory, see McEwan (1973) and Teoh, Ivey & Imberger (1997). These experiments investigated the nonlinear interaction of overlapping wave beams. Had the theory to be described here been available then, a single paddle producing overlapping beams of known linear behaviour may have been a suitable wave generator.

In § 2 the fluid is assumed to be inviscid and it is shown that the stream function describing the fluid motions can be expressed as a linear combination of the quadratic terms of the general solution derived in Part 1. In § 3 the Fourier decomposition of this stream function is modified by including in the integrands factors to account for viscous dissipation as was done in Part 2. The resulting solution is referred to as the approximate viscous one.

An exact solution of the viscous equations, expressed in terms of a distribution of

† Dr Hurley died on 5th February 2000 before the final revision of the paper.

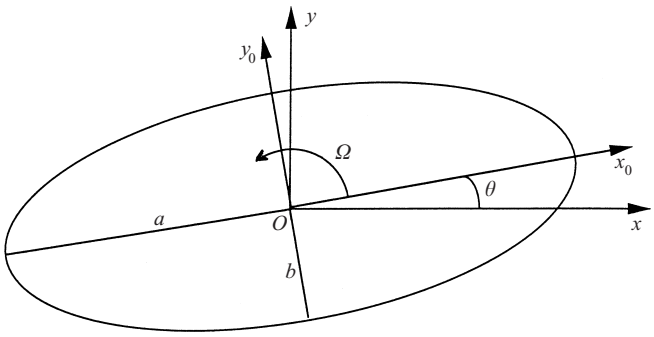

FIGURE 1. Notation.

semi-vortices, is then derived. This solution does not satisfy the boundary condition at the surface of the ellipse. However, it is shown that as the Reynolds number is increased it tends to the approximate viscous one which does satisfy the boundary condition in the limit of large Reynolds number.

The properties of the approximate viscous solution are investigated in §§ 4 and 5. It is shown that at large distances from the cylinder the solution for a beam of waves tends to a similarity one that decays with increasing distance more rapidly than does the similarity solution for rectilinear oscillations. Attention is then paid to regions near the cylinder where two beams of waves overlap. Finally the velocity profiles of the thin boundary layer adjacent to the cylinder are presented; they apply for both angular and rectilinear oscillations of the cylinder.

In § 6 the theories of Parts 1 and 2 are compared with recent experiments of Gavrilov & Ermanyuk (1997), Ermanyuk & Gavrilov (1999) and Sutherland *et al.* (1999).

2. Inviscid solution

We consider the internal gravity waves that are produced in an inviscid Boussinesq fluid of constant Brunt–Väisälä frequency N by an elliptic cylinder that is executing small angular oscillations at frequency ω about its centreline. The elliptic cross-section of the cylinder has semi-axes of lengths a and b and we suppose that the inclination of the a semi-axis to the horizontal is

$$\theta_i = \theta + \mathrm{i}\varepsilon \exp(-\mathrm{i}\omega t) \tag{2.1}$$

where $\varepsilon \ll 1$. The notation is shown in figure 1.

Differentiation of (2.1) gives

$$\frac{\mathrm{d}\theta_i}{\mathrm{d}t} = \Omega \exp(-\mathrm{i}\omega t), \tag{2.2}$$

where

$$\Omega = \epsilon\omega \tag{2.3}$$

is the amplitude of angular oscillations.

The fluid motion may be described in terms of a stream function $\psi(x, y)\exp(-\mathrm{i}\omega t)$ such that the velocity (u, v) is

$$u = -\frac{\partial\psi}{\partial y}\exp(-\mathrm{i}\omega t), \qquad v = \frac{\partial\psi}{\partial x}\exp(-\mathrm{i}\omega t), \tag{2.4}$$

with

$$\eta^2 \frac{\partial^2 \psi}{\partial x^2} - \frac{\partial^2 \psi}{\partial y^2} = 0, \tag{2.5}$$

where

$$\eta^2 = \frac{N^2}{\omega^2} - 1. \tag{2.6}$$

The boundary condition on the surface of the ellipse is (Milne-Thomson 1949)

$$\psi = \tfrac{1}{2}\Omega(x^2 + y^2) + B \tag{2.7}$$

where B is a constant.

We introduce the coordinates

$$\sigma_+ = x \sin\mu - y \cos\mu, \quad \sigma_- = x \sin\mu + y \cos\mu \tag{2.8}$$

where

$$\eta = \cot\mu. \tag{2.9}$$

In terms of them (2.5) is

$$\frac{\partial^2 \psi}{\partial \sigma_+ \partial \sigma_-} = 0, \tag{2.10}$$

whose general solution is

$$\psi = \psi_+(\sigma_+) + \psi_-(\sigma_-). \tag{2.11}$$

The expressions we take for ψ_+ and ψ_- in (2.11) are motivated by the work described in Part 1. There it was shown that the solution for an elliptic cylinder performing rectilinear oscillations could be expressed in the form (2.11) with

$$\psi_+ = c_+\alpha_+ \left[\frac{\sigma_+}{c_+} - \left(\frac{\sigma_+^2}{c_+^2} - 1\right)^{1/2}\right], \quad \psi_- = c_-\alpha_- \left[\frac{\sigma_-}{c_-} - \left(\frac{\sigma_-^2}{c_-^2} - 1\right)^{1/2}\right], \tag{2.12}$$

where

$$\left.\begin{aligned} c_+^2 &= a^2 \sin^2(\mu - \theta) + b^2 \cos^2(\mu - \theta), \\ c_-^2 &= a^2 \sin^2(\mu + \theta) + b^2 \cos^2(\mu + \theta). \end{aligned}\right\} \tag{2.13}$$

The straight lines $\sigma_+ = \pm c_+$ and $\sigma_- = \pm c_-$ are tangential to the ellipse as shown in figure 2 and the square roots in equations (2.12) take the values shown in figure 3 of Part 1. The constants α_+ and α_- in (2.12) were determined by satisfying the boundary condition on the surface of the ellipse that is appropriate for its performing rectilinear oscillations.

From the general solution derived in Part 1, for an ellipse performing angular oscillations the appropriate forms for ψ_+ and ψ_- are

$$\psi_+ = c_+\alpha_+ \left[\frac{\sigma_+}{c_+} - \left(\frac{\sigma_+^2}{c_+^2} - 1\right)^{1/2}\right]^2, \quad \psi_- = c_-\alpha_- \left[\frac{\sigma_-}{c_-} - \left(\frac{\sigma_-^2}{c_-^2} - 1\right)^{1/2}\right]^2 \tag{2.14}$$

where α_+ and α_- are determined by satisfying the boundary condition (2.7) on the ellipse.

In Hurley & Hood (2000) it is shown that the solution given by (2.11) and (2.14) does satisfy (2.7) if

$$B = -\tfrac{1}{4}\Omega(a^2 + b^2), \tag{2.15}$$

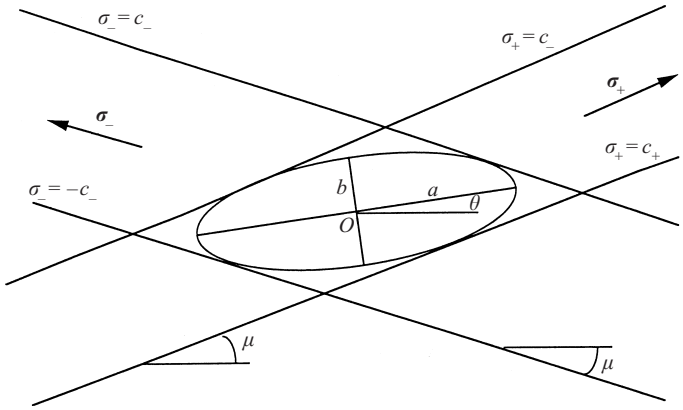

FIGURE 2. Notation.

$$\alpha_+ = \frac{\Omega c_+(a^2 - b^2)}{8(a\sin(\mu-\theta) + \mathrm{i}b\cos(\mu-\theta))^2} \tag{2.16}$$

and

$$\alpha_- = \frac{\Omega c_-(a^2 - b^2)}{8(a\sin(\mu+\theta) - \mathrm{i}b\cos(\mu+\theta))^2}. \tag{2.17}$$

(In Hurley & Hood 2000 the opportunity is taken to correct some minor errors in Parts 1 and 2.)

For waves in the first quadrant the dominant part of the fluid velocity is $(\partial\psi_+/\partial\sigma_+)\boldsymbol{\sigma}_+$ where ψ_+ is given by (2.14) and $\boldsymbol{\sigma}_+$ is a unit vector in the direction shown in figure 2. Also figure 3(a) of Part 1 gives

$$\begin{aligned}\left(\frac{\sigma_+^2}{c_+^2} - 1\right)^{1/2} &= \mathrm{i}\left(1 - \frac{\sigma_+^2}{c_+^2}\right)^{1/2}, \quad |\sigma_+| < c_+ \\ &= \pm\left(\frac{\sigma_+^2}{c_+^2} - 1\right)^{1/2}, \quad \pm\sigma_+ > c_+ \end{aligned} \tag{2.18}$$

where each of the bracketed quantities on the right-hand side of (2.18) denotes a positive quantity. Hence differentiation of (2.14) gives

$$\begin{aligned}\frac{1}{\alpha_+}\frac{\partial\psi_+}{\partial\sigma_+} &= \frac{4\sigma_+}{c_+} - 2\left(\frac{\sigma_+^2}{c_+^2} - 1\right)^{1/2} - \frac{2\sigma_+^2/c_+^2}{(\sigma_+^2/c_+^2 - 1)^{1/2}}, \quad \sigma_+ > c_+ \\ &= \frac{4\sigma_+}{c_+} - 2\mathrm{i}\left(1 - \frac{\sigma_+^2}{c_+^2}\right)^{1/2} + \frac{2\mathrm{i}\,\sigma_+^2/c_+^2}{(1 - \sigma_+^2/c_+^2)^{1/2}}, \quad c_+ > \sigma_+ > -c_+ \\ &= \frac{4\sigma_+}{c_+} + 2\left(\frac{\sigma_+^2}{c_+^2} - 1\right)^{1/2} + 2\frac{\sigma_+^2/c_+^2}{(\sigma_+^2/c_+^2 - 1)^{1/2}}, \quad \sigma_+ < -c_+. \end{aligned} \tag{2.19}$$

Using results in Erdelyi *et al.* (1954) we find that the Fourier decomposition of (2.19) is

$$\frac{1}{\alpha_+}\frac{\partial\psi_+}{\partial\sigma_+} = 2\mathrm{i}\int_0^\infty \left(J_0(K) - 2\frac{J_1(K)}{K}\right)\exp\left(\mathrm{i}K\frac{\sigma_+}{c_+}\right)\mathrm{d}K. \tag{2.20}$$

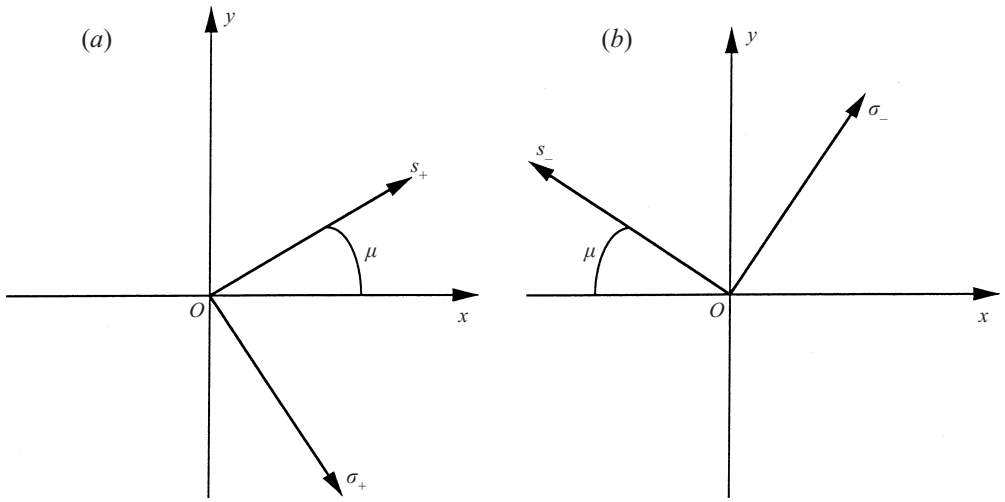

FIGURE 3. Notation: (*a*) $O\sigma_+s_+$ axes, (*b*) $O\sigma_-s_-$ axes.

Hence

$$\frac{\psi_+}{2c_+\alpha_+} = -\int_0^\infty \frac{J_2(K)}{K} \exp\left(\mathrm{i}K\frac{\sigma_+}{c_+}\right) \mathrm{d}K, \tag{2.21}$$

using the identity

$$\frac{2J_1(K)}{K} = J_0(K) + J_2(K).$$

The results for the dominant parts of waves in the other quadrants corresponding to (2.21) are found to be

$$\frac{\psi_+}{2c_+\alpha_+} = \mp\int_0^\infty \frac{J_2(K)}{K} \exp\left(\pm\mathrm{i}K\frac{\sigma_+}{c_+}\right) \mathrm{d}K \tag{2.22}$$

for waves in the 1st/3rd quadrants and

$$\frac{\psi_-}{2c_-\alpha_-} = \mp\int_0^\infty \frac{J_2(K)}{K} \exp\left(\mp\mathrm{i}K\frac{\sigma_-}{c_-}\right) \mathrm{d}K \tag{2.23}$$

for waves in the 2nd/4th quadrants.

2.1. *Calculation of power radiated and couple acting on cylinder*

The time average of the power per unit length of cylinder radiated in the first quadrant is

$$\bar{P}_1 = \frac{1}{4}\int_{-\infty}^{\infty} \left(p\left(\frac{\partial\psi_+}{\partial\sigma_+}\right)^* + p^*\left(\frac{\partial\psi_+}{\partial\sigma_+}\right)\right) \mathrm{d}\sigma_+ \tag{2.24}$$

where by (3.38) of Part 1

$$p = \mathrm{i}\rho_0\omega\eta\left\{c_+\alpha_+\left[\frac{\sigma_+}{c_+} - \left(\frac{\sigma_+^2}{c_+^2} - 1\right)^{1/2}\right]^2 - c_-\alpha_-\left[\frac{\sigma_-}{c_-} - \left(\frac{\sigma_-^2}{c_-^2} - 1\right)^{1/2}\right]^2\right\} \tag{2.25}$$

and an asterisk denotes the complex conjugate. Calculations using (2.19) and (2.24) show that non-zero contributions to $\bar{P}_1$ are confined to the portion of the line for

which $|\sigma_+| < c_+$ and that

$$\bar{P}_1 = \frac{\pi\rho_0\omega\eta\Omega^2(a^2-b^2)^2}{64}. \tag{2.26}$$

The total power radiated will be $4\bar{P}_1$ and we find that the instantaneous couple per unit length of cylinder acting on the cylinder to produce this power is

$$C = \frac{\pi}{8}\rho_0\omega\Omega\eta(a^2-b^2)^2\cos\omega t. \tag{2.27}$$

3. Approximate viscous solution

The approximate viscous solution is derived from the inviscid solution described above by using the procedure described in § 3 of Part 2. We include in the integrands of (2.22) and (2.23) above factors to account for viscous dissipation. Thus, we take

$$\psi_+ = \mp 2c_+\alpha_+ \int_0^\infty \frac{J_2(K)}{K} \exp\left(\mp K^3\lambda_+\frac{s_+}{c_+} \pm \mathrm{i}K\frac{\sigma_+}{c_+}\right) \mathrm{d}K, \quad \pm s_+ > 0, \tag{3.1}$$

$$\psi_- = \mp 2c_-\alpha_- \int_0^\infty \frac{J_2(K)}{K} \exp\left(\mp K^3\lambda_-\frac{s_-}{c_-} \mp \mathrm{i}K\frac{\sigma_-}{c_-}\right) \mathrm{d}K, \quad \pm s_- > 0, \tag{3.2}$$

where

$$\lambda_+ = \frac{\nu}{2c_+^2\omega\eta}, \quad \lambda_- = \frac{\nu}{2c_-^2\omega\eta}, \tag{3.3}$$

ν is the kinematic viscosity, and

$$\lambda_+ = \frac{1}{2\eta R_+}, \tag{3.4}$$

where

$$R_+ = \frac{c_+^2\omega}{\nu} \tag{3.5}$$

is a Reynolds number and there is a similar relationship between λ_- and R_-.

The s_+ and s_- are defined by

$$s_+ = x\cos\mu + y\sin\mu, \quad s_- = -x\cos\mu + y\sin\mu \tag{3.6}$$

and the $O\sigma_+s_+$ and $O\sigma_-s_-$ axes are shown in figure 3. However the definitions of s_+ and s_- must be slightly modified as described in Appendix B of Part 2.

For example (3.1) states that

$$\psi_+ = -2c_+\alpha_+ \int_0^\infty \frac{J_2(K)}{K} \exp\left(-K^3\lambda_+\frac{s_+}{c_+} + \mathrm{i}K\frac{\sigma_+}{c_+}\right) \mathrm{d}K, \quad s_+ > 0. \tag{3.7}$$

However, on the line $s_+ = 0$ this equation gives the inviscid values for ψ_+ and these are singular on the portion of the line $s_+ = 0$ for which $|\sigma_+| < c_+$ (see equation (3.37) of Part 1). Hence, except for the case of a circular cylinder, (3.7) will give values that have singularities in the flow field and is therefore unsatisfactory. However, it was shown at the end of Appendix B of Part 2, that if $\lambda \ll 1$ this deficiency can be overcome by taking the line $s_+ = 0$ to be to the left of the cylinder (see figure 8 of Part 2).

3.1. *Derivation of* (3.7) *from the exact viscous equations*

We focus attention on the beam of waves in the first quadrant when ψ_+ is given by (3.7) and satisfies (2.9) of Part 2, namely

$$\frac{\partial^2\psi_+}{\partial\sigma_+\partial s_+} + \frac{\mathrm{i}\nu}{2\omega\eta}\frac{\partial^4\psi_+}{\partial\sigma_+^4} = 0. \tag{3.8}$$

The exact equation for ψ_+ is equation (2.6) of Part 2, namely

$$\frac{\partial^2\psi_+}{\partial\sigma_+\partial s_+} + \cot 2\mu\frac{\partial^2\psi_+}{\partial s_+^2} + \mathrm{i}\frac{\nu}{2\omega\eta}\left(\frac{\partial^4\psi_+}{\partial\sigma_+^4} + 2\frac{\partial^4\psi_+}{\partial\sigma_+^2\partial s_+^2} + \frac{\partial^4\psi_+}{\partial s_+^4}\right) = 0. \tag{3.9}$$

We follow closely the procedure described in Appendix B of Part 2 and consider the inviscid case first.

3.1.1. *The inviscid case*

We take as our singular solution the semi-vortex given by

$$\psi_{V+}(\sigma_+) = \frac{1}{\pi}\log\sigma_+ = \mathrm{i}[1 - H(\sigma_+)] + \frac{1}{\pi}\log|\sigma_+|. \tag{3.10}$$

The Green's equivalent stratum for the present problem is proportional to the solution of the singular integral equation

$$\int_{-1}^{1}\frac{g(\tau'_+)\,\mathrm{d}\tau'_+}{\tau'_+ - \sigma'_+} = \sigma'_+, \quad -1 < \sigma'_+ < 1 \tag{3.11}$$

that satisfies the condition (see Hurley 1969)

$$\int_{-1}^{1} g(\sigma'_+)\,\mathrm{d}\sigma'_+ = 0, \tag{3.12}$$

where

$$\sigma'_+ = \frac{\sigma_+}{c_+}, \quad \tau'_+ = \frac{\tau_+}{c_+}, \quad \text{and subsequently } s'_+ = \frac{s_+}{c_+}. \tag{3.13}$$

Using results given in Carrier, Krook & Pearson 1966 we find that the solution of (3.11) and (3.12) is

$$g(\sigma'_+) = \frac{1 - 2\sigma_+'^2}{(1 - \sigma_+'^2)^{1/2}}. \tag{3.14}$$

It is then a straightforward matter to show using results in Erdélyi *et al.* (1954) that

$$\psi_+(\sigma'_+) = \frac{2\alpha_+c_+}{\pi}\int_{\Gamma_+}\frac{(1 - 2\tau_+'^2)\log(\sigma'_+ - \tau'_+)\,\mathrm{d}\tau'_+}{(1 - \tau_+'^2)^{1/2}} \tag{3.15}$$

where Γ_+ is the interval $(-1, 1)$ of the $O\tau'_+$ axis with an indentation below σ'_+, gives the velocities given by (2.19).

3.1.2. *The viscous case*

For the viscous solution we take

$$\psi_+^v = 2\alpha_+c_+\int_{\Gamma_+}\frac{(1 - 2\tau_+'^2)\psi_{V+}^v(\sigma'_+ - \tau'_+)\,\mathrm{d}\tau'_+}{(1 - \tau_+'^2)^{1/2}}, \tag{3.16}$$

where ψ^v_{V+} satisfies (B 9) of Appendix B of Part 2, namely

$$\frac{\partial^2\psi^v_{V+}}{\partial\sigma'_+ s'_+} + \cot(2\mu)\frac{\partial^2\psi^v_{V+}}{\partial\sigma'^2_+} + \mathrm{i}\lambda_+\nabla^4\psi^v_{V+} = -2\mathrm{i}\delta(\sigma'_+)\delta(s'_+). \tag{3.17}$$

We note that the homogeneous form of (3.17) is the exact equation (3.9). Hence ψ^v_+ given by (3.16) will also satisfy this exact equation except where $\sigma'_+ = \tau'_+$.

Equation (B 12) of Part 2 gives

$$\psi^v_{V+} \sim -\frac{1}{\pi}\int_0^\infty \frac{\exp(\mathrm{i}K\sigma'_+ - \lambda_+K^3 s'_+)}{K}\,\mathrm{d}K, \quad \lambda_+ \to 0. \tag{3.18}$$

Equations (3.16) and (3.18) now give

$$\psi^v_{V+} \sim -\frac{2\alpha_+c_+}{\pi}\int_0^\infty \frac{\exp(\mathrm{i}K\sigma'_+ - \lambda_+K^3 s'_+)}{K}\int_{\Gamma_+}\frac{(1-2\tau'^2_+)}{(1-\tau'^2_+)^{1/2}}\exp(-\mathrm{i}K\tau'_+)\,\mathrm{d}K\,\mathrm{d}\tau'_+, \quad \lambda_+ \to 0. \tag{3.19}$$

Carrying out the integral with respect to τ'_+ gives

$$\psi^v_+ \sim -2\alpha_+c_+\int_0^\infty \frac{J_2(K)}{K}\exp(-K^3\lambda_+ s'_+ + \mathrm{i}K\sigma'_+)\,\mathrm{d}K, \quad \lambda_+ \to 0 \tag{3.20}$$

which is equation (3.7) above.

We conclude that as $\lambda_+ \to 0$ the exact solution (3.16) tends to the approximate one (3.7) almost everywhere throughout the flow field. Exceptions are the vanishingly small regions surrounding the points where the characteristics touch the ellipse, see end of § 4.3 of Part 2.

4. Properties of a beam of waves in the approximate viscous solution

We focus attention on the beam of waves in the first quadrant for which (3.7) gives

$$\frac{\partial\psi_+}{\partial\sigma_+} = -2\mathrm{i}\alpha_+\int_0^\infty J_2(K)\exp\left(-K^3\lambda_+\frac{s_+}{c_+} + \mathrm{i}K\frac{\sigma_+}{c_+}\right)\mathrm{d}K. \tag{4.1}$$

4.1. *Solution at large distances from the cylinder*

Defining a distance parameter

$$d = \lambda_+\frac{s_+}{c_+} \tag{4.2}$$

for large values of d the major contribution to the integral in (4.1) comes from small values of K so that we may replace $J_2(K)$ therein by $K^2/8$ to obtain

$$\frac{1}{\alpha_+}\frac{\partial\psi_+}{\partial\sigma_+} \sim \frac{-\mathrm{i}}{4}\int_0^\infty K^2\exp\left(-K^3 d + \frac{\mathrm{i}K\sigma_+}{c_+}\right)\mathrm{d}K, \quad d \to \infty. \tag{4.3}$$

On introducing the similarity parameter

$$\zeta = \frac{\sigma^+/c^+}{d^{1/3}} \tag{4.4}$$

(4.3) gives

$$\frac{1}{\alpha_+}\frac{\partial\psi_+}{\partial\sigma_+} \sim \frac{-\mathrm{i}}{4d}\int_0^\infty k^2\exp(-k^3 + \mathrm{i}k\zeta)\,\mathrm{d}k. \tag{4.5}$$

It is of interest to compare this similarity solution with that for rectilinear oscillations given by (4.7) of Part 2 and by Thomas & Stevenson (1972), which can be written

$$\frac{1}{\alpha_+}\frac{\partial \psi_+}{\partial \sigma_+} \sim \frac{1}{2d^{2/3}} \int_0^\infty k \exp(-k^3 + ik\zeta)\, dk. \tag{4.6}$$

The similarity parameter is the same for both cases but for angular oscillations the fluid velocities decay more rapidly with distance from the ellipse than do those for rectilinear oscillations. Rectilinear oscillations are dipolar; angular oscillations are quadripolar. In the distant zone $d \gg 1$ Lighthill (1978, p. 380) shows that the excitation becomes effectively compact due to viscous attentuation, and the higher the order of the multipole source the more rapid the decrease of wave velocities with distance.

4.2. *The normalized velocity profiles*

On the centreline of the beam $\sigma_+ = 0$ and (4.1) gives the centreline velocity (as a function of d)

$$\left| \frac{1}{\alpha_+}\frac{\partial \psi_+}{\partial \sigma_+} \right|_{\sigma_+=0} = 2 \int_0^\infty J_2(K) \exp(-K^3 d)\, dK. \tag{4.7}$$

We define the beam width to be $2c_w$ (as a function of d) where c_w is the smallest positive value for which the real part of $\partial \psi_+/\partial \sigma_+$ vanishes. That is,

$$\int_0^\infty J_2(K) \exp(-K^3 d) \sin\left(K \frac{c_w}{c_+}\right) dK = 0. \tag{4.8}$$

Values of the real and imaginary parts of the *normalized* velocity profiles $(\partial \psi_+/\partial \sigma_+)/|\partial \psi_+/\partial \sigma_+|_{\sigma_+=0}$ are given in figure 4 as functions of σ_+/c_w for a number of values of d. The figure shows in a remarkable way how the profiles change from the inviscid one (equation (2.19)) to the similarity one (equation (4.5)) as d increases from zero to infinity.

5. The velocities near the cylinder in the approximate viscous solution

For distances from the cylinder of order a or less the ψ_+ and ψ_- waves significantly overlap and the fluid velocities $\boldsymbol{v}$ are given by

$$\boldsymbol{v} = \frac{\partial \psi_+}{\partial \sigma_+}\boldsymbol{\sigma}_+ + \frac{\partial \psi_-}{\partial \sigma_-}\boldsymbol{\sigma}_- \tag{5.1}$$

where $\partial \psi_+/\partial \sigma_+$ and $\partial \psi_-/\partial \sigma_-$ are given by (3.1) and (3.2) and $\boldsymbol{\sigma}_+$ and $\boldsymbol{\sigma}_-$ are unit vectors as shown in figure 2.

We consider the simple and instructive case $\theta = 0$ and $b = 0$ when the ellipse becomes a horizontal flat plate of length $2a$. In this case $c_+ = c_- = a \sin \mu$ and $\lambda_+ = \lambda_- = \lambda$, say. We focus attention on the triangular region bounded by the upper surface of the plate and the lines $\sigma_+ = -a \sin \mu$ and $\sigma_- = a \sin \mu$. Figure 4 shows how the values of $\partial \psi_+/\partial \sigma_+$ tend to the inviscid values as the Reynolds number R increases. Hence when $R \gg 1$ the values of $\partial \psi_+/\partial \sigma_+$ and $\partial \psi_-/\partial \sigma_-$, will be close to the inviscid values, whose Cartesian components (u, v) are found, using equation (2.19) to be

$$u = 2\alpha \cos \mu \left\{ 2(\sigma'_+ - \sigma'_-) + \frac{1 - 2\sigma'^2_+}{(\sigma'^2_+ - 1)^{1/2}} - \frac{(1 - 2\sigma'^2_-)}{(\sigma'^2_- - 1)^{1/2}} \right\}, \tag{5.2}$$

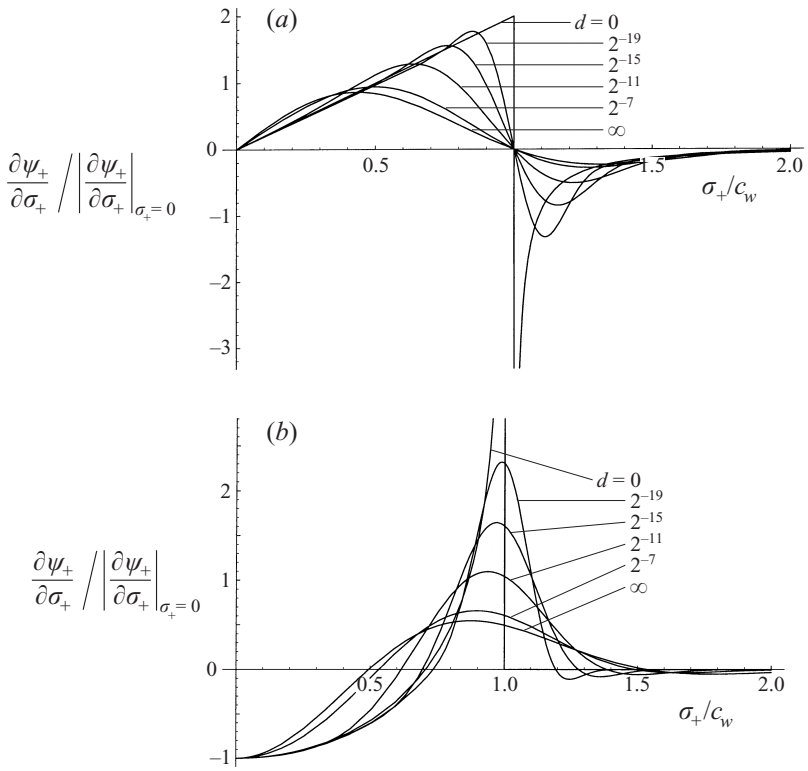

FIGURE 4. The normalized velocity profiles $(\partial\psi_+/\partial\sigma_+)/|\partial\psi_+/\partial\sigma_+|_{\sigma_+=0}$: (*a*) real part; (*b*) imaginary part.

$$v = 2\alpha \sin\mu \left\{ 2(\sigma'_+ + \sigma'_-) + \frac{1 - 2\sigma'^2_+}{(\sigma'^2_+ - 1)^{1/2}} + \frac{(1 - 2\sigma'^2_-)}{(\sigma'^2_- - 1)^{1/2}} \right\}, \tag{5.3}$$

where $(\sigma'^2_+ - 1)^{1/2}$ and $(\sigma'^2_- - 1)^{1/2}$ take the values given in figure 3 of Part 1. Also

$$\alpha = \frac{\Omega a}{8 \sin\mu}, \quad \sigma'_+ = x' - \eta y', \quad \sigma'_- = x' + \eta y'$$

where

$$x' = x/a \quad \text{and} \quad y' = y/a. \tag{5.4}$$

On the upper surface of the plate

$$u = \frac{-4\mathrm{i}\alpha \cos\mu (1 - 2x'^2)}{(1 - x'^2)^{1/2}} \tag{5.5}$$

and

$$v = 8\alpha x' \sin\mu, \tag{5.6}$$

an expression that will be needed in the next section.

5.1. *The oscillatory boundary layer on the surface of the plate*

We continue consideration of the case when $\theta = 0$ and $b = 0$ when the ellipse becomes a horizontal flat plate. We suppose that the fluid is slightly viscous and will investigate the oscillatory boundary layer that develops above the surface of the plate.

The governing boundary-layer equation is (Schlichting 1968, p. 411)

$$\frac{\partial u}{\partial t} - \nu \frac{\partial^2 u}{\partial y'^2} = \frac{\partial U(x')}{\partial t} \tag{5.7}$$

where ν is assumed to be constant and $U(x')$ is the velocity at the surface of the plate given by inviscid theory. Hence by (5.5)

where
$$\left.\begin{aligned} U(x') &= \mathrm{i}g(x'), \\ g(x') &= -4\alpha \frac{\cos \mu(1-2x'^2)}{(1-x'^2)^{1/2}}. \end{aligned}\right\} \tag{5.8}$$

Again following Schlichting we introduce the coordinate system Ox^*y^* linked to the plate with Ox^* along its surfaces. For a point close to the plate the difference between the velocities and accelerations relative to the Oxy and Ox^*y^* axes will be in the direction perpendicular to the plate. Hence the governing boundary-layer equation will be (5.7) with (x', y') replaced by (x^*, y^*). Hence it is

$$u^* - \frac{\mathrm{i}\nu}{\omega} \frac{\partial^2 u^*}{\partial y^{*2}} - \mathrm{i}g(x^*) = 0. \tag{5.9}$$

Also it follows from (5.5) and (5.6) that the boundary conditions are

$$u^* = 0 \quad \text{on} \quad y^* = 0 \tag{5.10}$$

and

$$u^* \to \mathrm{i}g(x^*) \quad \text{as } y^* \to \infty. \tag{5.11}$$

The solution of (5.9) which satisfies the boundary conditions is

$$u^* = \mathrm{i}g(x^*) \left[1 - \exp\left(\frac{-\xi}{2^{1/2}}\right) \exp\left(\frac{\mathrm{i}\xi}{2^{1/2}}\right)\right] \tag{5.12}$$

where

$$\xi = y^* \left(\frac{\omega}{\nu}\right)^{1/2}. \tag{5.13}$$

On multiplying by $\exp(-\mathrm{i}\omega t)$ and taking real parts we obtain

$$u^*(\xi, \omega t) = g(x^*) \left\{\sin \omega t - \exp\left(\frac{-\xi}{2^{1/2}}\right) \sin\left(\omega t - \frac{\xi}{2^{1/2}}\right)\right\}, \tag{5.14}$$

where $g(x^*)$ is given by (5.8).

Values of $u^*(\xi, \omega t)/g(x^*)$ for successive values of ωt are given in figure 5. We note that as $\xi \to \infty$, $u^* \to g(x^*) \sin \omega t$, the tangential velocity at the surface of the plate as given by inviscid theory.

Let us define the outer edge of the viscous boundary layer to be at $\xi = y^*(\omega/\nu)^{1/2} = 4$, that is at $y^* = 4(\nu/\omega)^{1/2}$. Then since the length scale for the variations in the velocities in the inviscid solution near the plate is a we have by (5.23) and (5.24) that at $y^* = 4(\nu/\omega)^{1/2}$

$$v^* \doteq 0, \quad u^* \doteq g(x^*) \sin \omega t, \tag{5.15}$$

or in other words that the inviscid boundary condition is approximately satisfied at the outer edge of the boundary layer if the inequality $(\nu/\omega)^{1/2} \ll a$ is satisfied. By (3.4) and (3.5) this inequality can be written

$$\lambda \ll 1. \tag{5.16}$$

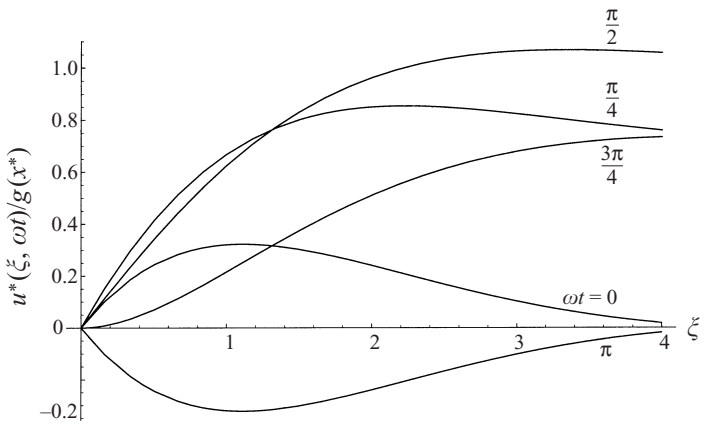

FIGURE 5. Velocity profiles of the oscillatory boundary layer on a horizontal plate for successive values of ωt. (See (5.14).)

Hence if (5.17) is satisfied we may, to leading order in λ, replace the viscous boundary condition at the surface of the plate by the inviscid one.

This conclusion clearly holds for all ellipses performing either angular or rectilinear oscillations. For example, consider a circular cylinder performing horizontal oscillations at speed U. Using results given in the Appendix of Part 1 we find that the tangential fluid velocity at the surface of the cylinder given by inviscid theory is

$$u_t = -\frac{U(\sin\mu + \mathrm{i}\cos\mu)\sin 2\varphi}{2\cos(\mu-\varphi)\cos(\mu+\varphi)}, \tag{5.17}$$

where φ is the angular coordinate of a point on the surface of the cylinder. The preceding analysis holds with u given by (5.5) replaced by u_t given by (5.18).

6. Comparison of theories with recent experiments

6.1. *Circular motion of the cylinder*

In a recent paper Gavrilov & Ermanyuk (1997) describe experiments on a circular cylinder whose centre is performing circular translational motions whose radius ε is small compared to the radius of the cylinder a. They observed the very interesting result that if the motion of the centre is in the clockwise direction the internal waves are generated only in quadrants I and III and not in quadrants II and IV.

We now investigate if these results are consistent with the theory of Parts 1 and 2, which was based on the assumption that all time-dependent quantities had time variation $\exp(-\mathrm{i}\omega t)$. Since only real parts have physical meaning, in particular

$$\text{stream function} = \mathrm{Re}\,\Psi(x,y,t) \tag{6.1}$$

where

$$\Psi(x,y,t) = \psi(x,y)\exp(-\mathrm{i}\omega t) \tag{6.2}$$

and $\psi(x,y)$ is a complex valued function. Equation (3.42) of Part 1 can be written

$$\psi(x,y) = a\alpha_+\left\{\frac{\sigma_+}{a} - \left(\frac{\sigma_+^2}{a^2}-1\right)^{1/2}\right\} + a\alpha_-\left\{\frac{\sigma_-}{a} - \left(\frac{\sigma_-^2}{a^2}-1\right)^{1/2}\right\} \tag{6.3}$$

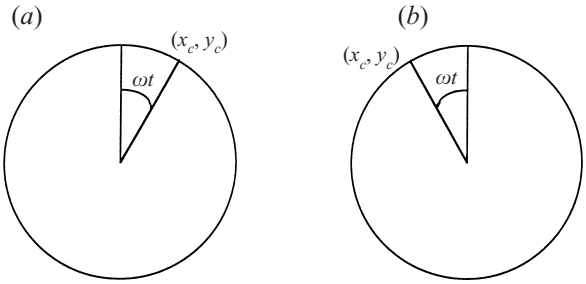

FIGURE 6. Position of the centre of a cylinder executing circular motion: (*a*) clockwise rotation; (*b*) anti-clockwise rotation.

where

$$\alpha_+ = \tfrac{1}{2}\{V\sin\mu + U\cos\mu + \mathrm{i}(V\cos\mu - U\sin\mu)\} = \tfrac{1}{2}(U + \mathrm{i}V)\exp(-\mathrm{i}\mu) \tag{6.4}$$

$$\alpha_- = \tfrac{1}{2}\{V\sin\mu - U\cos\mu + \mathrm{i}(V\cos\mu + U\sin\mu)\} = \tfrac{1}{2}(-U + \mathrm{i}V)\exp(-\mathrm{i}\mu). \tag{6.5}$$

(U, V) is the velocity of the cylinder, μ the inclination of the characteristics to the horizontal and

$$\sigma_+ = x\sin\mu - y\cos\mu, \quad \sigma_- = x\sin\mu + y\cos\mu. \tag{6.6}$$

Also the values of the square-roots in (6.3) are given figure 3 of Part 1.

Now suppose that in the experiments the centre of the cylinder, having coordinates (x_c, y_c), is describing in a clockwise direction at angular velocity $\omega < N$, a circle of radius $\varepsilon \ll a$. Suppose that at $t = 0$, $x_c = 0$ and $y_c = \varepsilon$. Then

$$x_c = \varepsilon\sin\omega t, \quad y_c = \varepsilon\cos\omega t, \tag{6.7}$$

$$\dot{x}_c = \omega\varepsilon\cos\omega t, \quad \dot{y}_c = -\omega\varepsilon\sin\omega t. \tag{6.8}$$

In these equations ωt is the angle between the Oy-axis and the current position of P the centre of the cylinder. (See figure 6*a*.)

Equation (6.8) shows that the horizontal and vertical motions are out-of-phase. However (6.3) was based on the assumption that U and V were in phase. Hence a direct application of (6.3) will not give the combined motions being considered.

First we determine the motion due to $\dot{x}_c = \omega\varepsilon\cos\omega t$ using (6.3) by taking $U = \omega\varepsilon$ and $V = 0$. Denoting the resulting stream function by $\psi_1(x, y)$ we have

$$\psi_1(x,y) = \frac{a}{2}\omega\varepsilon\exp(-\mathrm{i}\mu)\left[\left\{\frac{\sigma_+}{a} - \left(\frac{\sigma_+^2}{a^2} - 1\right)^{1/2}\right\} - \left\{\frac{\sigma_-}{a} - \left(\frac{\sigma_-^2}{a^2} - 1\right)^{1/2}\right\}\right]. \tag{6.9}$$

To determine the motion due to $\dot{y}_c = -\omega\varepsilon\sin\omega t$, we note that it can be written $\dot{y}_c = \omega\varepsilon\cos(\omega t + \pi/2) = \mathrm{Re}\{\omega\varepsilon\exp(-\mathrm{i}(\omega t + \pi/2))\}$. Hence denoting the consequent stream function by a subscript 2 we have from (6.1) that

$$\begin{aligned}\Psi_2(x,y,t) &= \psi_2(x,y)\exp(-\mathrm{i}(\omega t + \pi/2)) \\ &= -\mathrm{i}\psi_2(x,y)\exp(-\mathrm{i}\omega t)\end{aligned} \tag{6.10}$$

where $\psi_2(x, y)$ is given by (6.3) with $U = 0$ and $V = \omega\varepsilon$. Thus

$$\psi_2(x,y) = \frac{a}{2}\omega\varepsilon\mathrm{i}\exp(-\mathrm{i}\mu)\left[\left\{\frac{\sigma_+}{a} - \left(\frac{\sigma_+^2}{a^2} - 1\right)^{1/2}\right\} + \left\{\frac{\sigma_-}{a} - \left(\frac{\sigma_-^2}{a^2} - 1\right)^{1/2}\right\}\right]. \tag{6.11}$$

Hence the stream function for the combined horizontal and vertical motions of the cylinder is the real part of

$$\Psi(x,y,t) = (\psi_1(x,y) - \mathrm{i}\psi_2(x,y))\exp(-\mathrm{i}\omega t)$$
$$= a\omega\varepsilon\exp(-\mathrm{i}\mu)\left\{\frac{\sigma_+}{a} - \left(\frac{\sigma_+^2}{a^2} - 1\right)^{1/2}\right\}\exp(-\mathrm{i}\omega t), \tag{6.12}$$

using equations (6.9) to (6.11).

Equation (6.12) gives the σ_+ waves in quadrants I and III and shows that the σ_- ones in quadrants II and IV vanish. Hence the theory of Parts 1 and 2 is consistent with the experiments of Gavrilov & Ermanyuk.

The experiments described by Gavrilov & Ermanyuk showed that when the centre of the cylinder is rotating in the clockwise direction (as viewed from a point on the axis of the cylinder) there are no waves in quadrants II and IV. When the same experiment is viewed from the opposite end of the cylinder, the cylinder is rotating in the anti-clockwise direction and there are no waves in quadrants I and III.

6.2. *The experiments of Ermanyuk & Gavrilov (1999)*

The paper describes meticulous experiments on the internal waves produced by a circular cylinder oscillating in a horizontal direction. Oscillations of amplitudes as small as 0.5 mm were used.

They show in figures 2 and 3 that the experimental results compare favourably with theoretical predictions of Parts 1 and 2.

6.3. *The experiments of Sutherland et al.*

The paper describes an interesting new instrument, 'the synthetic schlieren', for investigating the motions occurring in a stratified fluid and contain a valuable set of experimental results for a circular cylinder executing vertical oscillations. The experimental results were in agreement with the theory of Parts 1 and 2.

7. Conclusions

7.1. *Angular oscillations*

We have described an extension of Parts 1 and 2 that described an investigation of the internal waves that are generated by an elliptic cylinder performing rectilinear oscillations to the case when the cylinder is performing angular oscillations about its centre.

The assumptions that must be satisfied in both cases for the results to hold are:

(i) that the flow is laminar everywhere and that no flow separations occur;

(ii) that $\lambda = 1/2\eta R \ll 1$ where $R = a^2\omega/\nu$ is the Reynolds number (see § 3);

(iii) that $V/\omega a$ is small where V is a typical velocity of a point on the surface of the ellipse.

It was found that at large distances from the cylinder the solution tends to a similarity one that decays more rapidly with increasing distance from the cylinder than does the similarity solution for rectilinear oscillations. Close to the cylinder the solution tends to the inviscid one as the Reynolds number is increased except in a thin viscous boundary layer that forms on the surface of the cylinder. Across this boundary layer the fluid velocities change from the values given by inviscid theory to those given by the no-slip boundary condition at the surface of the ellipse. The

velocity profiles in the boundary layer are presented. The results described in this paragraph clearly also hold for all ellipses performing either angular or rectilinear oscillations.

7.2. *Comparison of theories with recent experimental observations*

In all the experiments the Reynolds number was high and the cross-section of the cylinder was circular. The centre of the cylinder performed rectilinear oscillations in either the vertical or the horizontal direction, or circles of small radius. In the last case, beams of waves were observed in only two quadrants. This result is predicted by the theory of Parts 1 and 2. The other experimental results were in accord with the predictions of the theory of Parts 1 and 2.

The author wishes to acknowledge the suggestions of a reviewer which have improved the presentation of the paper.

REFERENCES

Carrier, G. F., Krook, M. & Pearson, C. E. 1966 *Functions of a Complex Variable*. McGraw-Hill.

Erdélyi, A., Magnus, W., Oberhettinger, F. & Tricomi, F. G. 1954 *Tables of Integral Transforms*, Vol. 1. McGraw-Hill.

Ermanyuk, E. V. & Gavrilov, N. V. 1999 Evaluation of added mass and damping of a circular cylinder oscillating in a linearly stratified fluid of limited depth. In *Proc. Workshop on Nonlinear Waves and their Interaction with Rigid Bodies* (*January 1999*). *Research Institute for Appl. Mech. Kyushu University, Rep.* 10 ME-S3, pp. 6–13.

Gavrilov, N. V. & Ermanyuk, E. V. 1997 Internal waves generated by circular translational motion of a cylinder in a linearly stratified fluid. *J. Appl. Mech. Tech. Phys.* **38**, 224–227.

Hurley, D. G. 1969 The emission of internal waves by vibrating cylinders. *J. Fluid Mech.* **36**, 657–672.

Hurley, D. G. 1997 The generation of internal waves by vibrating elliptic cylinders. Part 1. Inviscid solution. *J. Fluid Mech.* **351**, 105–118.

Hurley, D. G. & Hood, M. J. 2000 The generation of internal waves by vibrating elliptic cylinders. Part 3. Angular oscillations and comparison of theories with recent experimental observations. *Research Rep.* 2000/16. Department of Mathematics and Statistics, University of Western Australia.

Hurley, D. G. & Keady, G. 1997 The generation of internal waves by vibrating elliptic cylinders. Part 2. Approximate viscous solution. *J. Fluid Mech.* **351**, 119–138.

Lighthill, J. 1978 *Waves in Fluids*. Cambridge University Press.

McEwan, A. D. 1973 Interactions between internal gravity waves and their traumatic effects on a continuous stratification. *Boundary-Layer Met.* **5**, 159–175.

Milne-Thomson, L. M. 1949 *Theoretical Hydrodynamics*. Macmillan.

Schlichting, H. 1968 *Boundary-Layer Theory*. McGraw-Hill.

Sutherland, B. R., Dalziel, S. B., Hughes, G. O. & Linden, P. F. 1999 Visualisation and measurement of internal waves by 'synthetic schlieren'. Part 1. Vertically oscillating cylinder. *J. Fluid. Mech.* **390**, 93–126.

Teoh, S. G., Ivey, G. N. & Imberger, J. 1997 Laboratory study of the interaction between two internal wave rays. *J. Fluid Mech.* **336**, 91–122.

Thomas, N. H. & Stevenson, T. N. 1972 A similarity solution for viscous internal waves. *J. Fluid Mech.* **54**, 495–506.